Journal of Magnetic Resonance **140,** 363–370 (1999)
Article ID jmre.1999.1842, available online at http://www.idealibrary.com on IDEAL®

Mapping Brain Metabolites Using a Double Echo-Filter Metabolite Imaging (DEFMI) Technique

Wei Chen*,[1] and Jiani Hu†

**Center for Magnetic Resonance Research, Radiology Department, University of Minnesota, School of Medicine, Minneapolis, Minnesota 55455; and †MR Center, Harper Hospital, Wayne State University, Detroit, Michigan 48201*

Received November 18, 1998, revised March 17, 1999

A double echo-filter metabolite imaging (DEFMI) technique was developed for spatial mapping of low-concentration metabolites in the human brain. This imaging technique simultaneously acquires two images from two individual metabolites, respectively, using conventional imaging acquisition. It provides (i) efficient water and lipid suppressions, (ii) the capability of collecting high-resolution metabolite images within a short time and creating a ratio image from two interesting metabolites within a single experiment, and (iii) flexibility and simplicity for experimental setup and data processing. The technique was examined by both phantom and human brain experiments at 4 Tesla. The results reveal that the DEFMI technique is promising for applications in metabolism studies aimed at investigating physiological and pathological questions.

Key Words: **NMR spectroscopy; metabolite imaging; NMR sensitivity; chemical shift imaging; human brain.**

INTRODUCTION

The technique of chemical shift imaging (CSI) or spectroscopic imaging (SI) (*1–3*) is useful for noninvasively determining spatial distributions of various chemical species in living tissues under both physiological and pathological conditions. The conventional CSI technique uses phase-encoding gradients along two orthogonal dimensions combined with a slice selection and acquires free induction decays (FIDs) during an evolution period in the absence of gradients. Fourier transformation of FIDs yields a three-dimensional image (two spatial dimensions and one chemical shift dimension).

During the past decade, ^{1}H CSI had shown promise for mapping low-concentration metabolites by taking advantage of the high sensitivity of the proton nucleus and many existing techniques for suppressing extremely intensive water and lipid signals. The information from CSI is useful for determining metabolic abnormalities in the diseased brain. One of the most important findings from the brain disease studies using ^{1}H CSI and/or localized ^{1}H spectroscopy is the low concentration ratio of *N*-acetylaspartate (NAA) versus choline (Cho) and creatine (Cr) in the seizure foci of epilepsy compared to normal tissues (*4–8*). Early studies also demonstrated that NAA could be an important marker of neuronal viability (*9*) and that the ratio of [NAA]/([Cr] + [Cho]) was significantly correlated with glucose metabolism in temporal lobe epilepsy patients (*10*). These results suggest that the technique of using ^{1}H CSI for measuring the spatial distribution of [NAA]/[Cho] (or [NAA]/[Cho + Cr]) may provide a diagnostic tool for the evaluation of epilepsy and other diseases in patients.

However, the capability of the conventional CSI technique for routine clinical diagnosis is limited by several technical constraints: (i) long acquisition time (usually 30–60 min) due to low metabolite concentration and low NMR signal-to-noise ratio (SNR), (ii) relatively low spatial resolution and potential contamination of the residue lipid signals into the brain tissue due to spatial blurring, and (iii) complex post-data processing and relatively intensive computation for creating metabolite images. It would be useful to develop a robust and fast technique for mapping the spatial distributions of specific metabolites of interest. Many relevant techniques have been developed. One interesting category of these techniques uses frequency-selective pulses to excite a desired chemical shift range which only covers the resonances from the metabolites of interest (*11, 12*). When the bandwidth of the frequency-selective pulse is narrow enough to cover only one resonance peak, the multistep phase-encoding gradients along one spatial dimension used in CSI can be replaced by a one-step frequency-encoding gradient (*13, 14*). This gives a single metabolite image acquired the same way as in conventional MRI. The main advantages of using this technique are short acquisition time, simple data processing, straightforward image display, and capability for achieving high spatial resolution within a short time. Recently, an echo-filter technique using a narrow band frequency-selective refocusing pulse combined with dephasing gradients in a spin echo sequence has been developed for imaging a single metabolite. It has been used successfully to obtain NAA images in the human brain at 1.5 Tesla with excellent suppression of other resonance peaks including

[1] To whom correspondence should be addressed at Center for Magnetic Resonance Research, University of Minnesota School of Medicine, 2021 Sixth St. S.E., Minneapolis, MN 55455. Fax: (612) 626-2004. E-mail: wei@cmrr.umn.edu.

1090-7807/99 $30.00

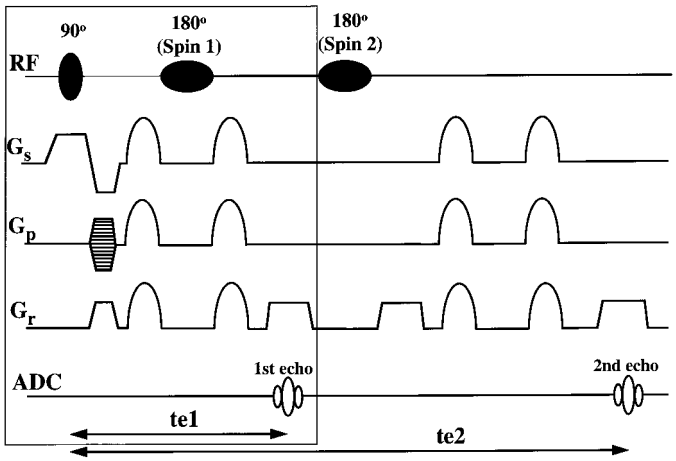

FIG. 1. Schematic presentation of the DEFMI pulse sequence. The first part of this pulse sequence depicted by the box is for single echo-filter metabolite imaging. It consists of a 90° excitation pulse (Sinc waveform) with slice selection gradient (G_s); phase-encoding gradient (G_p); the echo-filter 180° pulse (Gaussian waveform) for frequency-selective refocusing of spin 1; dephasing gradients (half-sine waveform) in three orientations; and readout gradient (G_r) for acquiring the first echo from spin 1. The second part of the sequence is for acquiring a second echo using another echo-filter 180° pulse for frequency-selective refocusing of spin 2. Outer volume signal and lipid contamination are suppressed by using the BISTRO OVS sequence prior to the sequence shown in this figure.

water and lipids (*14*). In this work, we have adapted a similar idea from the single metabolite imaging technique and expanded it to a novel technique of double echo-filter metabolite imaging (DEFMI) where two echoes from two desired metabolite resonances are collected in a single scan.

The DEFMI pulse sequence is demonstrated in Fig. 1. The first part of this pulse sequence, depicted by the box in Fig. 1, is used for acquiring single echo-filter metabolite imaging. It consists of a 90° excitation pulse with slice selection, phase-encoding gradient, the echo-filter 180° pulse for frequency-selective refocusing of only spin 1, dephasing gradients in three orientations, and a readout gradient for acquiring the first echo from spin 1. The second part of the sequence is for acquiring a second echo using another echo-filter 180° pulse for frequency-selective refocusing of only spin 2. The dephasing gradients in the second part of the pulse sequence are designed for refocusing the second echo signal and dephasing the other multiecho signals generated from the first echo. This technique provides a fast spatial mapping of two metabolites of interest within the same experiment. Taking advantage of high sensitivity and high spectral resolution at high magnetic fields, the technique has been examined by both phantom and human brain experiments at 4 Tesla to show its capability of creating two separated metabolite images with close chemical shifts and the ratio images of metabolites in the human brain.

The DEFMI technique also provides a full sensitivity for detecting the water-exchangeable protons in the low-field region (e.g., N-H protons and aromatic C-H protons coupled to N-H groups). This is achieved by avoiding the magnetization transfer signal loss due to water saturation for solvent suppression purposes used for most CSI techniques (*15, 16*). It was demonstrated that the signal intensity of the resonance peak at 8.3 ppm, which is tentatively assigned to nucleosides and protein, is sensitive to pH changes in the brain tissue (*15*). Therefore, the sensitivity gain achieved by the DEFMI technique is important for spatial mapping of the 8.3-ppm resonance peak that may indirectly provide the brain pH and other physiological information.

RESULTS

Figure 2 demonstrates the lactate and NAA images acquired simultaneously using the DEFMI technique from the multicompartment phantom (see Experimental). The frequency-selective refocusing pulses were set at 1.3 ppm for lactate and 2.0 ppm for NAA, respectively. The intense water signal from the phantom was completely suppressed and the locations of the lactate and NAA images were well separated and consistent with the anatomical images from the bottles in the multicompartment phantom. Figure 3a shows the spectra acquired from Cr and Cho, respectively, using the DEFMI sequence (single scan and entire slice) in the human brain. High SNR, efficient suppression of other undesired signals, and good separation of the Cr and Cho resonances (0.17 ppm difference) were achieved by taking advantage of the high sensitivity and spectral resolution at 4-Tesla high magnetic field. The excellent water (4.7 ppm) and lipid (~1.3 ppm) suppressions were obtained by the echo-filters and outer-volume suppression (OVS) without using other water and lipid suppression techniques. These are important for obtaining individual metabolite images with minimal contamination from other resonance signals and for improving reliability of metabolite quantification. Figure 3b shows a Cr metabolite image from a representative subject. A high spatial resolution (nominal spatial resolution = 0.2 cm^3) was obtained within a relatively short acquisition time (12.8 min) using the DEFMI technique. The Cr metabolite image shows the spatial contrast of the Cr content between the gray matter and white matter (depicted by the solid line in Fig. 3b) by comparing the Cr metabolite image and the T_1-weighted gradient-echo image. The Cr intensity in the gray matter is higher than that in the white matter and the $[Cr]_{white}/[Cr]_{gray}$ ratio is 0.80 based on the comparison of the average Cr intensity between 88 white matter pixels (depicted by the black boxes in Fig. 3b) and 83 gray matter pixels (depicted by the white boxes in Fig. 3b). This ratio is in agreement with the result (0.80) of another study using CSI (*17*). Figure 4 demonstrates the feasibility of the DEFMI technique for obtaining the Cr (the first echo) and NAA (the second echo) metabolite images simultaneously acquired in a single experiment and creating the [NAA]/[Cr] ratio image within the brain tissue. Nominal spatial resolution was 0.39 cm^3 and total acquisition time was 8.5 min.

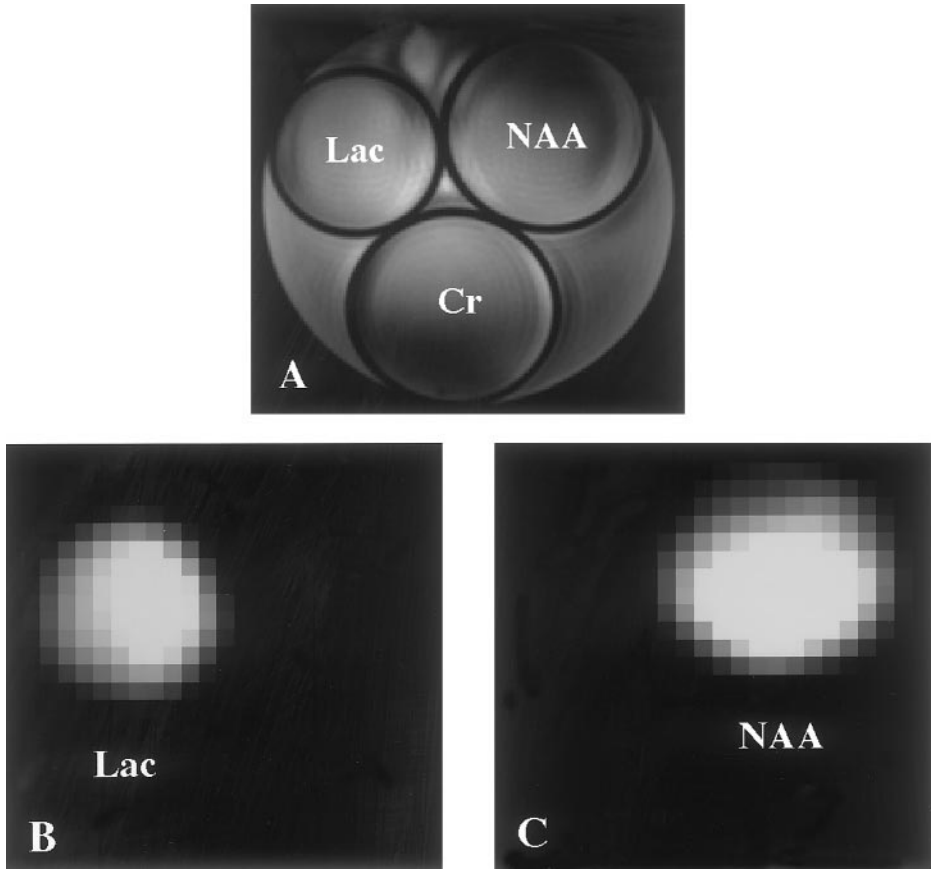

FIG. 2. (A) Transverse scout image of the multicompartment phantom, (B) the lactate, and (C) NAA images acquired simultaneously using the DEFMI technique (TR = 3 s, 2.4-min acquisition). The frequency-selective refocusing pulses were set at 1.3 ppm for lactate (Lac) and 2.0 ppm for NAA, respectively.

Figure 5 shows the spectra of the entire human brain slice acquired by the DEFMI sequence where the echo-filter refocusing pulse was centered at 8.3 ppm (A) without and (B) with CHESS water suppression (*18, 19*). Substantial signal loss at 8.3 ppm (~50%) is evident due to the magnetization transfer effect induced by presaturation CHESS pulses. The difference spectrum in Fig. 5C shows an approximately symmetric single peak at 8.3 ppm whereas the right shoulder peak at 8 ppm (tentatively assigned to NAA) is canceled by the spectral subtraction. Twofold signal gain using the DEFMI technique allowed obtainment of the high-resolution metabolite image of the 8.3-ppm resonance peak and the ratio image relative to Cr as demonstrated in Fig. 6 from another individual subject.

DISCUSSION

Our results demonstrate that the DEFMI technique is capable of achieving complete water suppression and well-separated individual metabolite images between two close resonance peaks and creating metabolite ratio images in the human brain. The replacement of one-dimensional phase-encoding gradient by frequency-encoding gradient in the DEFMI sequence significantly reduces the total acquisition time for acquiring metabolite images and makes it possible to obtain high-resolution metabolite images within a short time. An excellent SNR achieved at 4 Tesla provides a well-defined contrast of Cr signal between the gray and white matters on the metabolite image (Fig. 3) with a very high spatial resolution (0.2 cm^3) and relatively short imaging time (<13 min). Other advantages are simple and fast data processing and imaging display that are identical to the conventional MRI. These make it possible to examine results during metabolite imaging studies.

There are different T_2 weightings between the first and second echoes collected for metabolite images due to different echo times. The T_2 signal losses can be corrected if the T_2 values of the two metabolites are known. One of the main differences between the DEFMI technique and conventional CSI is the correction factor due to different echo times and T_2 values of metabolites. The inhomogeneity of the static magnetic field (B_0) is relatively poor over the entire slice (e.g., 14–20 Hz at 4 Tesla). This can cause a slight offset between the metabolite resonance peak and the echo-filter (frequency-selective refocusing pulse) profile peak inside a pixel and lead to an attenuation of the pixel signal intensity. Therefore, the

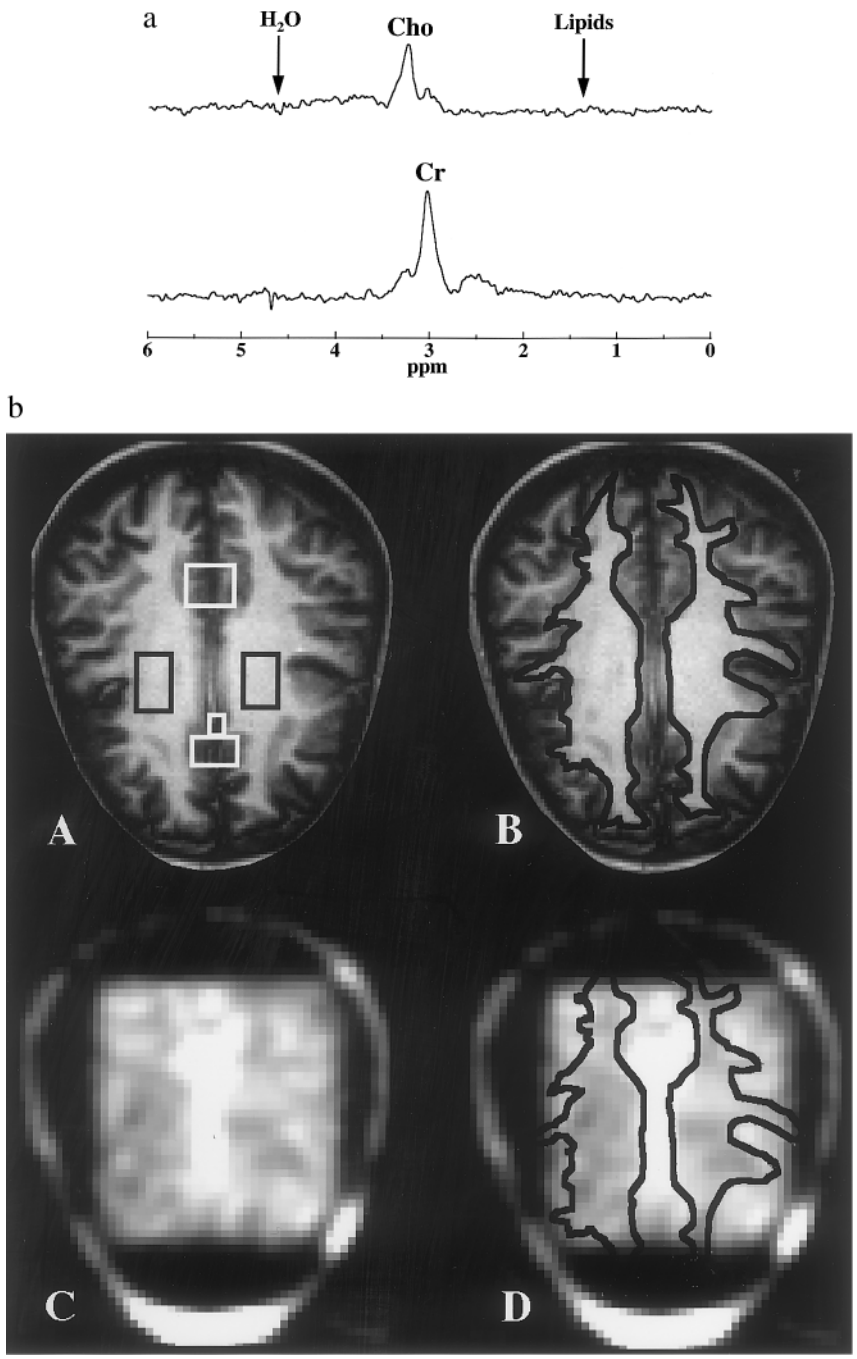

FIG. 3. (a) ^{1}H spectra acquired from individual Cr and Cho peaks, respectively, using the DEFMI sequence (single scan and entire slice) from a representative subject. The creatine and choline resonances are well separated. Complete water (4.7 ppm) and lipid (~1.4 ppm) suppressions were achieved by the echo filters and OVS. (b) T_1-weighted gradient-echo image (A and B) and the Cr metabolite image (C and D). A high spatial resolution Cr metabolite image (nominal spatial resolution = 0.2 cm^3, 20 × 20-cm^2 FOV, 64 × 32 matrix size interpolated to 64 × 64, eight averages) was obtained with a 12.8-min acquisition time. The Cr metabolite image shows the spatial contrast of Cr concentration between the gray matter and white matter approximately separated by the solid line in B and D.

signal intensity of the metabolite image depends on not only the metabolite concentration but also B_0, B_1 distributions, and other pulse sequence parameters. However, the signal variations do not cause significant problems for quantifying metabolite ratio images because of the compensation between two metabolite signal intensities within the same pixel. This improves the reliability for determining metabolic concentration ratios. The resonance peaks of lipid compounds in tissues can partially overlay with the NAA resonance peak. The overlaid lipid peaks can be detected together with the NAA peak.

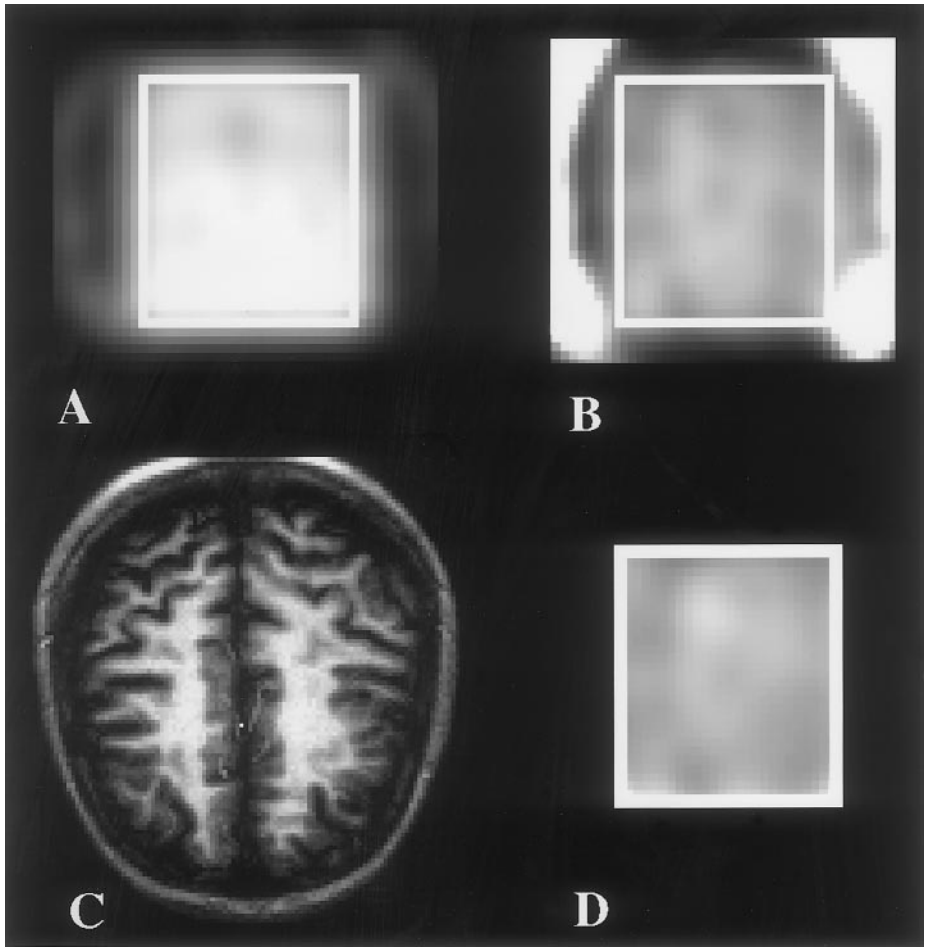

FIG. 4. (A) Cr and (B) NAA metabolite images simultaneously acquired by the DEFMI technique in a single experiment from a representative subject. (C) T_1-weighted gradient-echo image and (D) the [NAA]/[Cr] ratio image within the brain tissue (depicted by the boxes in A and B). The nominal spatial resolution for the Cr and NAA metabolite images was 0.39 cm^3 and the total acquisition time was 8.5 min (40 × 20-cm^2 FOV, 64 × 32 matrix size interpolated to 128 × 64, eight averages).

However, the lipid signals are spatially differentiated from the NAA signal inside the brain tissue as shown in Fig. 4. The high spatial image resolution significantly reduces the spatial blurring of the lipid signal into the brain tissue.

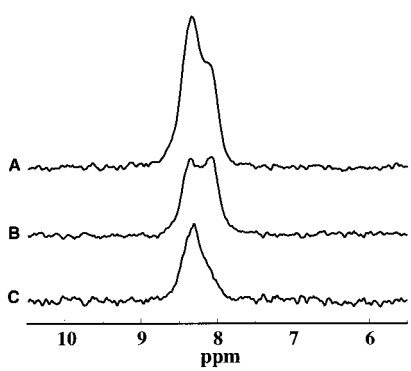

FIG. 5. ^{1}H spectra of a brain slice acquired by the DEFMI sequence (16 scans), where the echo-filter refocusing pulse was centered at 8.3 ppm, (A) without and (B) with CHESS water suppression. (C) The difference spectrum between A and B.

Several techniques have been proposed for obtaining separated water and lipid images in humans (*20–22*). These techniques work well in the simple case where only two intense resonances are assumed and the chemical shift difference between the two resonances is large (e.g., water versus lipid). In comparison with these techniques, the DEFMI technique provides a much narrower frequency selection for separating two close resonance peaks and the echo-filter provides excellent suppression of undesired resonances. This makes it possible to obtain metabolite images with extremely low concentration and minimal contamination from other resonances including water and lipids. However, the capability of the DEFMI method for separating two close resonance peaks can be limited, especially at low magnetic field due to lower spectral resolution. At 4 Tesla, the Cr (or Cho) resonance peak detected by the DEFMI technique contains ~20% signal contributed by Cho (or Cr). This can lead to an overestimation of image signal intensity. Increasing the echo-filter pulse widths can reduce this limitation at the expense of T_2 signal loss because of longer echo time.

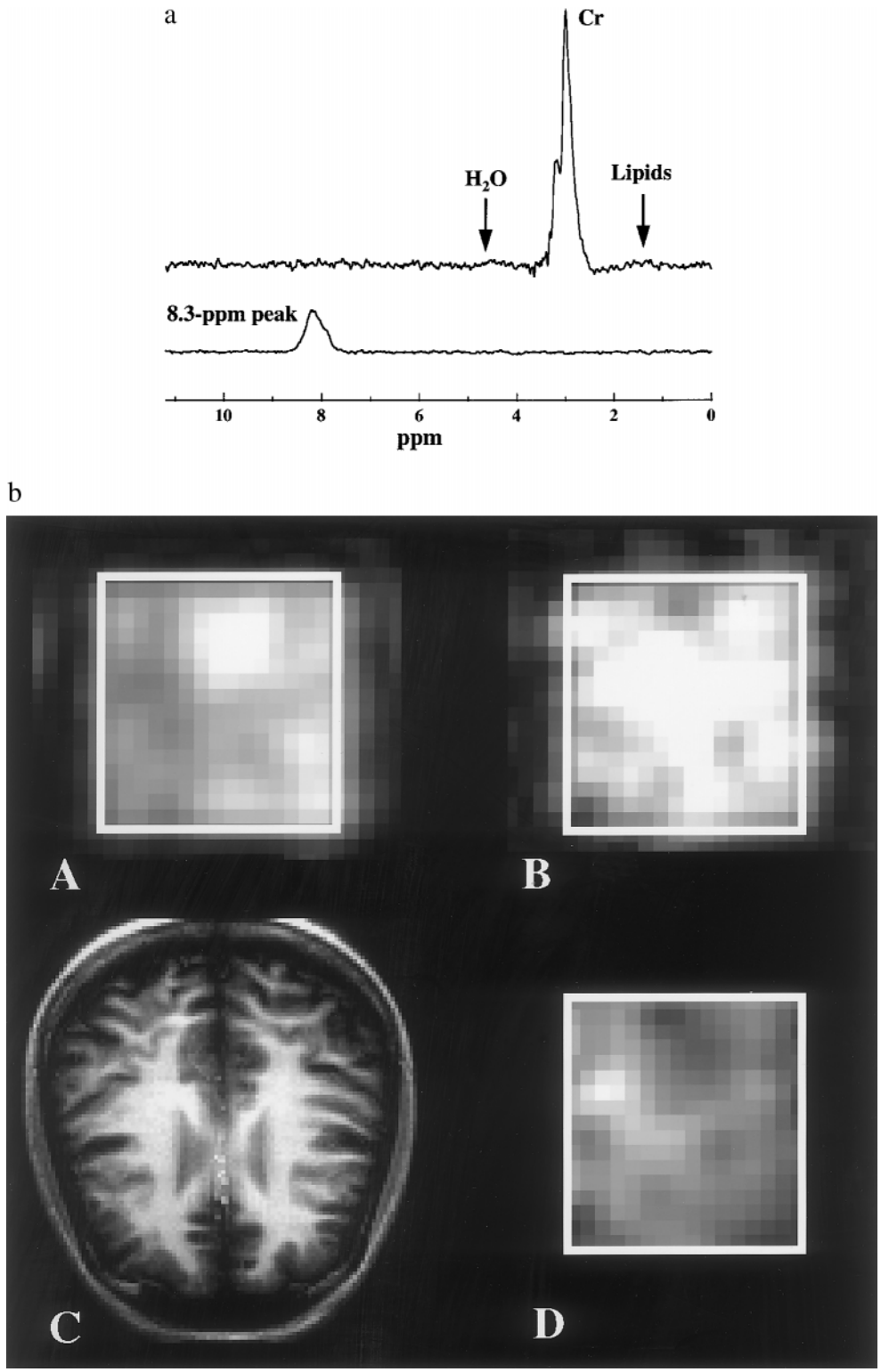

FIG. 6. (a) ^{1}H spectra acquired from Cr peak (one scan) and 8.3-ppm resonance peak (eight scans), respectively, using the DEFMI sequence (entire brain slice) from a representative subject. The same vertical display scales were used. Both peaks are well defined with minimal water and lipid contamination. (b) The Cr (A) and 8.3-ppm (B) metabolite images simultaneously acquired by the DEFMI technique in a single experiment from a representative subject; T_1-weighted gradient-echo image (C) and the [8.3-ppm]/[Cr] ratio image within the brain tissue (D). The nominal spatial resolution of the metabolite images was 0.78 cm^3 and the total acquisition time was 6.4 min (20×20-cm^2 FOV, 32×16 matrix size interpolated to 32×32, eight averages). The image display scale in B was multiplied by 3 compared to A.

The DEFMI technique is useful for detecting lactate and some other (homonuclear) coupled spins without the effect of J-coupling evolution which can lead to dephasing and signal loss, because only one of the two coupled spin groups is refocused. Thus, the T_2 maps of these metabolites can also be measured.

Finally, our results show the promising application of the DEFMI technique for imaging the spatial distributions of the water-exchangeable protons at 8.3 ppm. The symmetric lineshape of the difference spectrum as shown in Fig. 5 indicates that the difference peak may be mainly contributed by a single resonance at 8.3 ppm. In addition to the pH dependence (*15*), the signal intensity of the 8.3-ppm resonance is sensitive to the brain tumor based on the human brain CSI study (*16*). Therefore, the metabolite image from this resonance may provide physiological information about the human brain.

CONCLUSIONS

A robust technique using the DEFMI sequence for metabolite mapping was developed. The results demonstrate the feasibility of the technique to obtain two metabolite images in a single experiment. The DEFMI technique provides (i) the capability for obtaining high-resolution metabolite images within a short time; (ii) flexibility and simplicity for experimental setup, data processing, and interpretation; and (iii) a robust imaging technique to create a reliable ratio image from two interesting metabolites which can reflect the metabolite concentration ratio if the T_2 correction is calculated. The technique may have potential applications for mapping metabolites and metabolite concentration ratios in normal and pathological brain studies and in routine clinical diagnosis.

EXPERIMENTAL

All NMR experiments were performed on a 4-Tesla Siemens/Varian whole-body system equipped with a head gradient insert. A quadrature birdcage coil was used for transmitter and receiver at 170 MHz. Five healthy subjects without history of neurological disorders recruited from the academic university environment participated in this study that was approved by the institutional review board of the University of Minnesota Medical School.

A radio frequency (RF) pulse with Sinc waveform was used for slice selection in the axial orientation (2-ms pulse width and 1-cm slice thickness). A Gaussian RF pulse (20-ms pulse width) was used for the echo-filter refocusing pulses. It had a 76-Hz bandwidth (0.45 ppm at 4-Tesla magnetic field strength) at the half-maximum excitation peak value. This narrow bandwidth allows refocusing of a single resonance peak and suppression of other resonance peaks with different chemical shifts via the strong dephasing gradients. BISTRO (B_1-insensitive selective train to obliterate signal) pulse trains were employed before the pulse sequence as shown in Fig. 1 for OVS by taking advantages of its high suppression efficiency, low RF power requirement, B_1 insensitivity, and a sharper saturation profile (*23, 24*). The BISTRO pulse trains were generated using a series of hyperbolic secant pulses (*25*) (2-ms pulse width) combined with slice selection and dephasing gradients. The OVS pulses were applied in two dimensions perpendicular to the slice selection direction and optimized to maximize outer volume signal suppression and minimize signal loss within a localized volume ($\sim 10 \times 10$ cm^2) inside the brain tissue. The echo times used in the DEFMI sequence were 37 and 104 ms for the first echo (te1) and second echo (te2), respectively. The repetition time (TR) was 2–3 s. The image acquisition times (at) were 8 ms. For human studies, the field of view (FOV) along the frequency-encoding direction was 20 cm [spectral width (SW) = 3871 Hz] or 40 cm (SW = 7742 Hz) with a 64-image matrix size and the FOV along the phase-encoding direction was 20 cm with a 32-image matrix size. The acquired raw data were Gaussian filtered in k-space before Fourier transformation for SNR enhancement. The metabolite images were interpolated to 64 or 128 pixel size by zero-filling. In addition, a relatively low resolution was used for studying the water-exchangeable resonance at 8.3 ppm (see details in the figure legend to Fig. 6). A multicompartment phantom consisting of three bottles having 10 mM lactate, NAA, and Cr, respectively, was used for testing the DEFMI sequence. The DEFMI sequence has options to collect a FID from spin 1 or spin 2 over the entire slice in the absence of gradients. This was used to examine the frequency selectivity for acquiring a single metabolite (SW = 5000 Hz, at = 205 ms, and TR = 3 s). Multislice T_1-weighted TurboFLASH images (128×128 matrix size, axial orientation and two segmentations) were acquired in all studies for anatomical information. Typical imaging parameters were 1.2-s inversion time (TI), 4.7-ms TE, 9.6-ms TR, 5-mm slice thickness, and 20×20-cm^2 FOV.

ACKNOWLEDGMENTS

The authors thank Drs. Kamil Ugurbil, Jeffrey L. Evelhoch, and Xiao-Hong Zhu for their support. This research was partially supported by P41 RR08079, a National Research Resource (NIH) grant, and NIH Grant NS38071 (W.C.).

REFERENCES

1. T. R. Brown, B. M. Kincaid, and K. Ugurbil, NMR chemical shift imaging in three dimensions, *Proc. Natl. Acad. Sci. USA* **79,** 3523–3526 (1982).
2. A. A. Maudsley, S. K. Hilal, H. E. Simon, and W. H. Perman, Spatially resolved high resolution spectroscopy by "four dimensional" NMR, *J. Magn. Reson.* **51,** 147–152 (1983).
3. X. Hu, W. Chen, M. Patel, and K. Ugurbil, Chemical shift imaging: An introduction to its theory and practice, *in* "Biomedical Engineering Handbook" (J. D. Bronzino, Eds.), pp. 1036–1045, CRC Press (1995).
4. J. W. Hugg, R. I. Kuzniecky, F. G. Gilliam, R. B. Morawetz, R. E. Fraught, and H. P. Hetherington, Normalization of contralateral

metabolic function following temporal lobectomy demonstrated by ^{1}H magnetic resonance spectroscopic imaging, *Ann. Neurol.* **40,** 236–239 (1996).

5. T. C. Ng, Y. G. Comair, M. Xue, N. So, A. Majors, H. Kolem, H. Luders, and M. Modic, Temporal lobe epilepsy: Presurgical localization with proton chemical shift imaging, *Radiology* **193,** 465–472 (1994).
6. F. Cendes, F. Andermann, M. C. Preul, and D. L. Arnold, Lateralization of temporal lobe epilepsy based on regional metabolic abnormalities in proton magnetic resonance spectroscopic imaging, *Ann. Neurol.* **35,** 211–216 (1994).
7. A. Connelly, G. D. Jackson, J. S. Duncan, M. D. King, and D. G. Gadian, Magnetic resonance spectroscopy in temporal lobe epilepsy, *Neurology* **44,** 1411–1417 (1994).
8. S. N. Breiter, S. Arroyo, V. P. Mathews, R. P. Lesser, R. N. Bryan, and P. B. Barker, Proton MR spectroscopy in patients with seizure disorders, *Am. J. Neuroradiol.* **15,** 373–384 (1994).
9. T. Ebisu, W. D. Rooney, S. H. Graham, M. W. Weiner, and A. A. Maudsley, *N*-Acetylaspartate as an *in vivo* marker of neuronal viability in kainate-induced status epilepticus: ^{1}H magnetic resonance spectroscopic imaging, *J. Cerebr. Blood Flow Metab.* **14,** 373–382 (1994).
10. D. Lu, C. Margouleff, E. Rubin, D. Labar, N. Schaul, T. Ishikawa, K. Kazumata, A. Antonini, V. Dhawan, and R. A. Hyman, Temporal lobe epilepsy: Correlation of proton magnetic resonance spectroscopy and ^{18}F-fluorodeoxyglucose positron emission tomography, *Magn. Reson. Med.* **37,** 18–23 (1997).
11. D. C. Shungu and J. D. Glickson, Band-selective spin echoes for *in vivo* localized ^{1}H NMR spectroscopy, *Magn. Reson. Med.* **32,** 277–284 (1994).
12. J. R. Alger, G. Brunetti, G. Nagashima, and K. A. Hossmann, Evaluation of a newly discovered water suppression pulse sequence for high-field *in vivo* ^{1}H surface coil NMR spectroscopy, *Magn. Reson. Med.* **11,** 73–84 (1989).
13. B. Mora, P. T. Narasimhan, B. D. Ross, J. Allman, and P. Barker, ^{31}P magnetization transfer and phosphocreatine imaging in the monkey brain, *Proc. Natl. Acad. Sci. USA* **88,** 8372–8376 (1991).
14. J. Hu and J. L. Evelhoch, Direct *in vivo* ^{1}H metabolite imaging: 0.35 cc NAA image of human brain less than 7 minutes at 1.5T, *in* "Proceedings, ISMRM, 4th Annual Meeting, New York, 1996," p. 1223.
15. S. Mori, S. M. Eleff, U. Pilatus, N. Mori, and P. C. van Zijl, Proton NMR spectroscopy of solvent-saturable resonances: A new approach to study pH effects *in situ, Magn. Reson. Med.* **40,** 36–42 (1998).
16. J. Hu, W. Chen, G. R. Barger, and J. L. Evelhoch, *In vivo* proton magnetic resonance spectroscopy of human brain in the aromatic region, *in* "Proceedings, ISMRM, 5th Annual Meeting, Vancouver, Canada, 1997," p. 1211.
17. H. P. Hetherington, G. F. Mason, J. W. Pan, S. L. Ponder, J. T. Vaughan, D. B. Twieg, and G. M. Pohost, Evaluation of cerebral gray and white matter metabolite differences by spectroscopic imaging at 4.1T, *Magn. Reson. Med.* **32,** 565–571 (1994).
18. A. Haase, J. Frahm, W. Hanicke, and D. Matthaei, ^{1}H NMR chemical shift selective (CHESS) imaging, *Phys. Med. Biol.* **30,** 341–344 (1985).
19. C. T. W. Moonen and P. C. M. van Zijl, Highly effective water suppression for *in vivo* proton NMR spectroscopy (DRY-STEAM), *J. Magn. Reson.* **88**(28–41) (1990).
20. J. A. B. Lohman, R. J. Ordidge, and A. Connelly, Spin echo imaging of multiple chemical shifts, *Magn. Reson. Med.* **5,** 83–86 (1987).
21. D. Kunz, Double pulse echoes—A novel approach for fat–water separation in magnetic resonance imaging, *Magn. Reson. Med.* **3,** 639–643 (1986).
22. W. T. Dixon, Simple proton spectroscopic imaging, *Radiology* **153,** 189–194 (1984).
23. Y. Luo, A. Tannus, and M. Garwood, Frequency-selective elimination of coherent signal with B_1 insensitivity: An improved outer-volume suppression method (BISTRO), *in* "Proceedings, SMR, 3rd Annual Meeting, Nice, France, 1995," p. 1017.
24. W. Chen, Y. Luo, H. Merkle, X.-H. Zhu, G. Adriany, M. Garwood, and K. Ugurbil, Low-power, B_1-insensitive, frequency-selective saturation pulse for use of water suppression and saturation transfer in NMR, *in* "Proceedings, SMR, 3rd Annual Meeting, Nice, France, 1995," p. 1016.
25. M. S. Silver, R. I. Joseph, and D. I. Hoult, Highly selective p/2 and p pulse generation, *J Magn. Reson.* **59,** 347–351 (1984).